Using GIS and Multicriteria Analysis to Map Flood Risk Areas of the Tongo Bassa River Basin (Douala, Cameroon)

Willy Sone Essoh[†], **Raphael Onguene**[‡], **Barthelemy Ndongo**[§], **Georges Nshagali**[††], **Antoine Colmet-Daage**[‡‡], **Guillaume Marie**[§§], **Junior Iroume**[‡], **Thomas Stieglitz**[†††], **Felix Besack**[†], **Thomas Efole Ewoukem**[†], **Minette Tomedi Eyango**[†], **Jacques Etame**[‡], and **Jean Jacques Braun**[‡‡‡]

[†]LERH, EDOSFA
University of Douala
Cameroon

[‡]LASAT, EDOSFA
University of Douala
Cameroon

[§]Department of Rural Engineering
FASA, University of Dschang
Cameroon

[††]Department of Geology
Official University of Bukavu
Rwanda

[‡‡]PHILIA Ingénierie
Toulouse, France

[§§]LDGIZC
Université du Québec à Rimouski
Canada

[†††]Aix Marseille University
CNRS, IRD, INRA, Coll France, Centre de Recherche et d'Enseignement de Géosciences de l'Environnement (CEREGE)
Aix-en-Provence 13545, France

[‡‡‡]Biology Pedagogy Centre
Centre National de la Recherche Scientifique (CNRS)
Vandaeuvre-lès-Nancy, Cedex 54501, France

www.cerf-jcr.org

ABSTRACT

Sone Essoh, W.; Onguene, R.; Ndongo, B.; Nshagali, G.; Colmet-Daage, A.; Marie, G.; Iroume, J.; Stieglitz, T.; Besck, F.; Efole Ewoukem, T.; Tomedi Eyango, M.; Etame, J., and Braun, J.J., 2023. Using GIS and multicriteria analysis to map flood risk areas of the Tongo Bassa River Basin (Douala, Cameroon). *Journal of Coastal Research, 39*(3), 531–543. Charlotte (North Carolina), ISSN 0749-0208.

The present study aimed to map the areas at risk of flooding in the Tongo Bassa watershed (42 km^2) located in the heart of the Cameroonian economic capital (Douala) in the tropical zone of Central Africa, more precisely in the Wouri Estuary, at the bottom of the Gulf of Guinea. Like most of the world's major cities, Douala is subject to floods. The methodological approach was to identify the flooding risk determinants in the area from an extensive literature review and field surveys and then analyze these factors and map areas at risk of flooding using the analytical hierarchy process approach coupled with the GIS environment. The results revealed that four parameters of the natural environment (elevation, drainage density, distance to the river, and land cover) were the factors that mainly influenced the phenomenon of flooding in the region. Three major classes of flood risk were highlighted: low risk, medium risk, and high risk. To validate the effectiveness of the flood risk map obtained, the flood points collected in the field were cross-checked for ground truth after a flood occurred in the watershed. This cross-check between the resulting map and the flood points using GIS tools showed a good representation of the flooded area. This result is quite interesting because the areas where the risk of flooding is high are consistent with those where flooding is most frequent. The presented results constitute a basic decision support tool for the management of flood zones by the public authorities and the decentralized territorial communities of the city of Douala.

ADDITIONAL INDEX WORDS: *Flood risk, hierarchical multicriteria analysis, Tongo Bassa, Douala, Cameroon.*

INTRODUCTION

Over the past two decades, the global frequency of floods has increased by more than 40% (Hirabayashi, Mahendran, and Koirala, 2013). Between 1995 and 2015, approximately 109 million people were affected by floods, with corresponding damages of up to $75 billion per year (Alfieri *et al*., 2017). A compilation of global floods by the United Nations Office for Disaster Risk Reduction indicates that 2887 floods were reported from 1980 to 2008, resulting in nearly 196,000 deaths, with an average of nearly 6873 deaths per year or nearly 68 people per event (Guha-Sapir *et al*., 2011).

Africa's vulnerability to hydro-climatic hazards is increased tenfold by the combination of several factors such as poverty, bad governance, the lack of infrastructure and adequate technology, ecosystem degradation, complex disasters, and conflicts (Ahouangan *et al*., 2010). The inefficiency of solid waste collection systems, the extension of buildings into flood-prone areas, and modest sanitation networks are also factors that aggravate the hazard. These reinforce the foreseeable effects of flood risks on highly impoverished urban populations (Issaka, 2010).

In Cameroon, floods are considered by experts to be the most frequent natural disaster. According to studies published by CRED (2016), 367,276 people were victims of floods between 2007 and 2015. The Littoral Region, most especially the city of Douala (the economic capital of Cameroon), is an example. Located at the bottom of the Gulf of Guinea, the city of Douala

is subject to the effects of the tides, which are felt more than 62 km from the mouth of the Wouri (Onguene *et al.*, 2014). Between 2000 and 2010, floods caused more than 100 deaths in Douala and significant material and human damage (Zogning, Tonye, and Tsalefack, 2015).

Douala has experienced significant population growth since colonial times, which intensified after independence (Mbaha, Olinga, and Tchiadeu, 2013; Nsegbe *et al.*, 2014). Estimated at 2.5 million inhabitants in 2010 (BUCREP, 2010; PDU, 2011), projections indicate that Douala will have between 1.3 and 1.6 million additional inhabitants in 2025, *i.e.* nearly 4 million. This growing population induces anarchic land use, and land access is now granted to the highest bidder. Most occupants do not have a valid building permit or land title.

Catastrophic floods are expected to become more frequent as a result of the trends in climate change combined with the increase in the population living on floodplains, deforestation, the disappearance of wetlands, and a rise in mean sea level, in the decades to come (IPCC, 2012). A significant number of people will therefore be exposed to this phenomenon. So far, there is no available map of flooded and flood risk areas, and this makes the issue of flood risk management increasingly worrying for governments and municipalities. This could explain the failure of most management measures put in place by the city managers regarding the heavy flood that occurred in the city of Douala on 21 August 2020, which resulted in significant material damage. This work aimed to produce a map of areas at risk of flooding using the hierarchical multicriteria analysis method developed by Saaty (1980) to help manage the risk of floods in the studied area.

Hydraulic and hydrological modelling approaches have been used by various researchers to provide flood susceptibility mapping (Matkan *et al.*, 2009; Merwade, Cook, and Coonrod, 2008). However, these methods require sufficient and accurate data (Fenicia *et al.*, 2013; Refsgaard, 1997). In the city of Douala, no detailed hydrological or hydraulic model has yet been applied because of the lack of available data and the complexity of the oceanographic phenomena that influence the city due to its position in the estuary area. Coupled Analyse Multi-critères (Multi-criteria analysis, AMC)-GIS approaches have been used in spatial modelling and natural hazard analysis (Malczewski, 2006; Paquette and Lowry, 2012; Scheuer, Haase, and Meyer, 2011; Solín, 2012).

Various studies have demonstrated that these techniques can be used to generate hazard maps (Akgun and Turk, 2010; Bui *et al.*, 2015; Emmanouloudis, Myronidis, and Ioannou, 2008; Kritikos and Davies, 2011; Sinha *et al.*, 2008). The analytical hierarchy process (AHP) (Saaty, 1980) is a popular technique in the field of multicriteria decision-making (Pourghasemi, Pradhan, and Gokceoglu, 2012; Rozos, Bathrellos, and Skillodimou, 2011). One of the main problems with the AHP method is the need to exploit expert knowledge in assigning weights, which can be considered a source of bias. However, the main goal of disaster management is to develop a transferable methodology that can be used globally (Tehrany *et al.*, 2014). The effectiveness of GIS and AMC was evaluated by Fernández and Lutz (2010) for mapping floodplains in the province of Tucumán, Argentina. Their

study indicated that the AHP technique in a GIS environment is a powerful method for generating flood hazard maps with a good degree of accuracy. Additionally, Zou *et al.* (2013) described AHP as an understandable, cost-effective, and practical method for flood risk assessment.

The purpose of this article is to propose a generally usable methodology carried out in the GIS environment that will determine the areas prone to flood risk. The result will be a basic tool that can better guide development projects and management measures by city managers.

METHODS

Conventional flood risk analysis methods use hydrological and hydraulic modelling approaches with field measurements or remote-sensing data used for model inputs (Arnaud and Lavabre, 2010). However, there is a growing trend to develop spatial models based on physical factors and their contribution rates to characterize flood risk (Lang and Lavabre, 2007).

Study Area

The Tongo Bassa is the largest watershed in the city of Douala with an area of 42 km^2 (Meva'a, Fouda, and Bonglam, 2010), and its outlet is the Wouri River. It runs through the city of Douala from E to W, and it is located between 4°2′0″ and 4°5′30″ N latitude and between 9°43′0″ and 9°47′20″ E longitude (Figure 1). This watershed is a wetland threatened by human populations with anarchic constructions subjected to floods (schools, several sanitary facilities, shopping centers, and roads). The slope of the land varies between 0.1% and 0.7% (Olinga, 2012), and it has a dendritic type hydrographic network with a constant flow throughout the year, characterized by water stagnation in the lowlands. The climate is hot and humid (equatorial type), characterized by temperatures between 21 °C and 36 °C with very abundant rainfall, which has been decreasing since 2007, *i.e.* 3593.5 mm on average monthly (Tchiadeu and Olinga, 2012). It is located in the agroecological part of Africa with monomodal rainfall, for which the climate is characterized by two seasons during the year (one rainy from March to November and the other dry from December to February) (Tchiadeu and Ketchemen-Tandia, 2009). Geologically, this watershed is dominated by sandy formations from the Miocene and Pliocene, which are very favorable to infiltration and rapid waterlogging of the soil (Boum-Nkot *et al.*, 2015). Above all, the water table is almost flush with the surface in the lower-elevation parts. Furthermore, the soil hydrodynamic tests carried out revealed low permeability on the slopes (Fouda and Meva'a, 2004). This reality is linked to the ferralitic nature of the predominantly yellowish and sometimes variegated sandy-clay soil. Therefore, the characteristics of the relief and the substrate, the hydrodynamics of the soils, and the hydrological regime are very favorable for the stagnation of surface waters (Meva'a, Fouda, and Bonglam, 2010).

The vegetation in this part is mainly mangrove forest, which provides a diversity of habitat and advantages such as the proximity to the sea, the soil nature, the drainage, the elevation, and opportunities for other activities, in this case, logging (Ajonina, 2006). In total, 27 neighborhoods make up
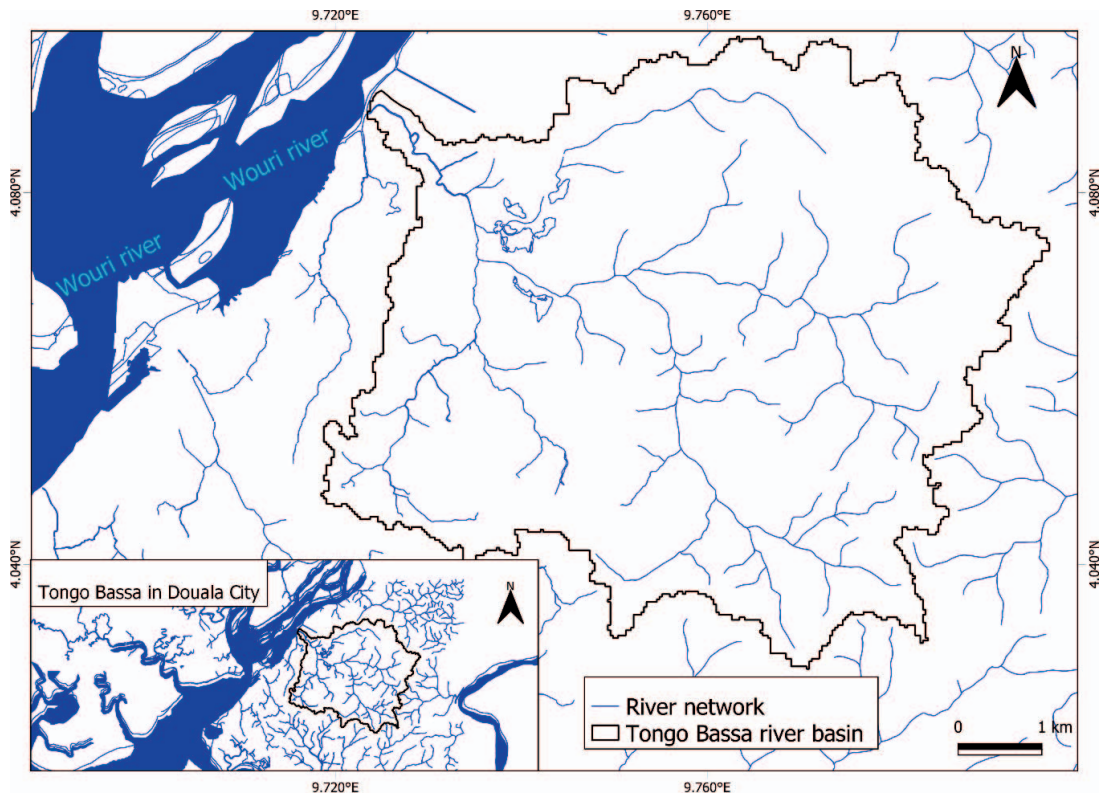
Figure 1. Presentation of study area, Tongo Bassa river basin, connected to the Wouri River Douala, Cameroon, and the density of the rivers contributing to the genesis of the floods in Douala.

the Tongo Bassa watershed, with population density ranging from 25 to more than 350 inhabitants/ha (Boum Nkot *et al.*, 2015).

The fluctuation of the tide in the Wouri Estuary causes the flows in the drains connected to it to vary because the drainage flow from the mainland to the river at high tide is very reduced (Ndongo *et al.*, 2015). Therefore, many areas are flooded during rain showers, and it appears that the stagnation of water from various sources is inevitable in Tongo Bassa.

Figure 2. Applied method synthesis and presentation of the major processing steps.

Data Sources

The topographic relief and the hydrographic network in the Tongo Bassa watershed were described from a Shuttle Radar Topography Mission (SRTM) image obtained from https://urs. earthdata.nasa.gov to determine the different levels of elevation in the watershed and its hydrography. From this, the drainage density was calculated, and the proximity of the human population and infrastructure to the different rivers was analyzed. For a better analysis of the land cover, Landsat 8 satellite images from the Operational Land Imager (OLI) satellite mission were obtained *via* the internet from the U.S. Geological Survey (USGS) website, which helped to make maps of land cover by supervised classification on the free Qgis GIS application. The treatment processes are described below (Figure 2). The flood points were recorded in the field by GPS geolocation directly after the flood of 21 August 2020.

Method Description

To carry out this study, two methods were used: (1) identifying the parameters that have more or less impact on the flooding phenomenon, which was done based on an intense literature review on the theme of floods coupled with several field observation campaigns and available data; and (2) mapping of flood risk areas using the AHP and a GIS environment. Last, the final result was validated using the flood points collected in the field after the 21 August 2020 flooding event (Figure 2).
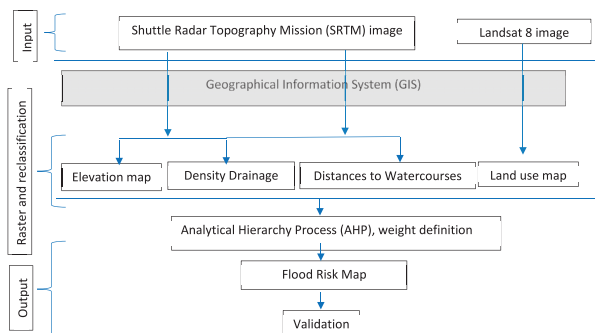
Flooding Identification Criteria

The identification of the criteria is a decisive and delicate phase that conditions the quality of the data generated with a view to their inclusion in the model. Thus, after reviewing the literature, prospecting the watershed, regarding the work of Jourda *et al.* (2006), Mahmoud and Gan (2018), Phonphoton and Pharino (2019), and Youan *et al.* (2011) and available data, four criteria were analyzed to meet the objective. The defined criteria were elevation, drainage density, distance to watercourses, and land use.

The elevation map was produced using the SRTM image at 30 m × 30 m spatial resolution. This map shows the different levels of elevation and indicates the low areas, which are the areas of water accumulation. The drainage density map was also produced using the SRTM image and shows areas of high river density. Where there is a greater density of rivers, there is a higher likelihood for overflow in the event of a flood. The watercourse distance map was also produced using the SRTM image. This was made by a succession of processing steps in the GIS environment and indicates the floods in the major beds of the rivers and their distances from populated areas.

The land cover map was produced from the satellite image of the Landsat 8 OLI sensor acquired in 2020. This map provides information on multiple issues in the catchment area, in this case, the built issues. These criteria were carefully selected to avoid redundancies and take into account the almost flat relief of the watershed.

To evaluate the contribution of each criterion to the susceptibility to flooding, criteria were pairwise correlated. For this purpose, the schematic sketch of Shaban *et al.* (2001) was used. Typically, one (1) point is assigned to a factor when it is dominant (major), and 0.5 point is assigned when it is minor (Hammami *et al.*, 2019; Saaty, 1980). The sum of the points obtained makes it possible to classify the parameters according to their importance in the susceptibility to flooding. This classification was then used for the AHP.

Analysis Hierarchy Process (AHP)

The AHP makes it possible to objectively determine weights or weighting coefficients by comparing factors taken two by two using a matrix. So, the first step is to define the decision problem. The second step consists of judging the relative importance of the criteria from the scale of Saaty (1980) and the development of the comparison matrix. It also allows the weighting coefficient to be determined from the eigenvectors of these criteria. Each criterion was given a numerical value between 1 and 9, depending on its importance. A numerical value of 1 means that the two factors being compared are of equal importance; a numerical value of 9 means that the row factor is much larger than the column factor.

After establishing the reasoning, a matched comparison matrix is formed for the different options deemed relevant. Then, normalization is conducted, in which the relative importance of the criteria classes is indicated. There are different methods of normalization, but the most popular is the eigenvector method. The eigenvector method uses an inverse, square matrix decomposition A, instead of the maximum eigenvalue ($\lambda_{\max}$):

Table 1. *Incompatibility index (IA) of random matrices for* N ≤ 10 *(Saaty, 1980).*

N	1	2	3	4	5	6	7	8	9	10
IA	0	0	0.58	0.9	1.12	1.24	1.32	1.41	1.45	1.45

$$\lambda max = \frac{1}{N} \sum_{i=1}^{N} \frac{Wj(Ai)}{Wi} \qquad (1)$$

where, A is the matched comparison matrix, W is the weight vector, and λ is the scalar (number), respectively. Once the option priority vectors have been provided for all the criteria, the calculations are repeated to prioritize and determine their weights until the highest hierarchical level is reached.

A compatibility check of the decision makers' judgments was carried out based on the relevant mathematical relationships. The results were studied according to the comparison matrices. Regarding the relation below, the matrix $A = [aij]$ will be compatible if the following relation holds between all elements (Ghodsipoor, 2006):

$$aik = aij \times ajk \rightarrow i, j, k = 1, 2, 3, \ldots, n \qquad (2)$$

where, $\lambda_{\max}$ is always greater than or equal to n. If the matrix moves a little away from the compatibility mode, $\lambda_{\max}$ will be a little away from n. Thus, the difference between $\lambda_{\max}$ and n (namely, $\lambda_{\max} - n$) can be a good reference with which to measure matrix incompatibility. The scale of $(\lambda_{\max} - n)$ depends on the value of n (the length of the matrix). It can be defined as follows to meet dependency, and this is called the consistency index (*CI*):

$$CI = \lambda_{\max} - n \;/\; n - 1 \qquad (3)$$

The control of the compatibility of the judgments of the decision makers was carried out based on indices of incompatibility. The values of the incompatibility index were calculated on matrices in which the numbers were completely randomized. This has been called the random incompatibility index (*IA*), and their values are equal in Table 1 for n-dimensional matrices.

The consistency ratio (*RC*) was obtained for each matrix based on the division of the consistency index (*CI*) over the random incompatibility index (*IA*), which is a good criterion for judging incompatibility matrices.

$$RC = CI \;/\; IA \qquad (4)$$

If the number is less than or equal to 0.1, then the compatibility of the systems can be accepted; otherwise, the judgments must be revised (Ghodsipoor, 2006).

Evaluation of the Contribution Rate of the Criteria

The database used for the mapping of areas at risk of flooding was previously processed in the free software QGIS 3.18. Each criterion map was produced in raster format with a size of 30 m × 30 m. From the dimensions assigned to each class of criteria, the "Reclassify raster" module was used to produce the layers (Ake *et al.*, 2018). The aggregation of the different layers using the "weighted overlay" module made it possible to establish the final flood risk map of the Tongo Bassa watershed. The iterative calculation of the resulting final map was performed
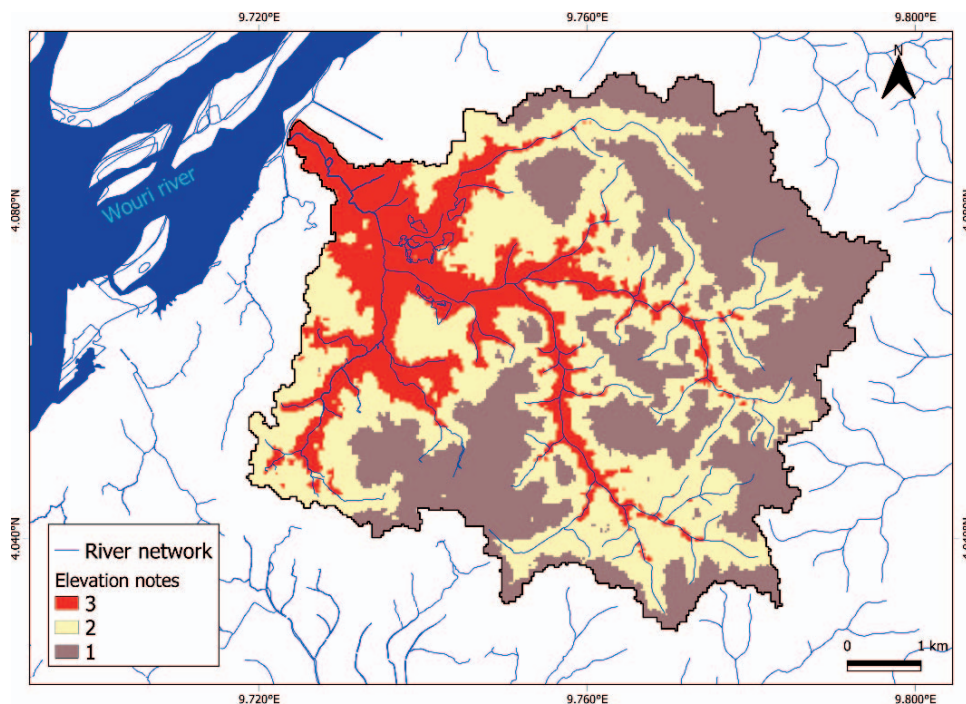
Figure 3. Elevation map, which presents ratings assigned to elevation classes in the watershed to describe the magnitude of flooding (1 = low; 2 = medium; 3 = high).

according to Equation (5) below:

$$S = \sum_i wixi \qquad (5)$$

where, S is the result or contribution (linear combination of criteria values, χ_i, weighted by weights, w_i), w_i is the weight of criterion i, and x_i is the criterion. The summary of the processing carried out is presented below (Figure 2).

Validation

The final map of areas at risk of flooding was validated with the flood points surveyed on the ground directly after the flood of 21 August 2020. After cross-checking the two pieces of information, the areas at high risk are better represented. Several authors (Daouda *et al.*, 2022; Lee, Kang, and Jeon, 2012; Mahmoud and Gan, 2018; Pradhan *et al.*, 2011; Tehrany *et al.*, 2014) have used statistical methods, in particular, the area under the curve (AUC), for validation because they have a lot of data and regularly integrate 10 criteria on average.

To represent the extent of the areas likely to be flooded for better flood management, this study shows that the flood points surveyed after an actual flood are quite sufficient for validation.

RESULTS

This part presents the results of the processing. It will describe in turn the criteria involved in the analysis model in order to better justify the map of areas at risk of flooding.

Analysis and Mapping of the Main Studied Criteria

In this study, four main criteria (elevation, drainage density, distance to watercourses, and land cover) were used to map the

flood zones in the Tongo Bassa watershed in Douala using the AHP. The results are presented in the form of tables and figures.

Elevation Map

Elevation plays a very important and effective role in flood susceptibility (Poussin and Botzen, 2014). Lower-elevation areas are more likely to be flooded, and low areas are the points of convergence of different streams (Rahman *et al.*, 2021). The Tongo Bassa watershed is laid out on almost flat terrain with elevations between 0 m and 60 m, for an average of 30 m. The map of elevations in the area is shown in Figure 3, where elevation has been subdivided into three classes ($\leq$10 m, 10–30 m, and >30 m) represented by the percentages: 0.63%, 0.26%, and 0.11%. These different classes were assigned grades 3, 2, and 1, respectively (Table 2).

Drainage Density Map

Drainage density is defined as the ratio of the total length of streams in a watershed to the area of the watershed. The higher the drainage density of an area is, the more likely it is to be flooded, which justifies its significant impact on the occurrence of floods (Kouassy *et al.*, 2019). The drainage density map shown in Figure 4 has been classified into three classes, with values ranging from 0 and 4.5 km/km^2. These values are high around watercourses and at confluences. Due to its significant contribution to the flooding process, the highest density class received a score of 3, while the lowest density class received a score of 1 (Table 2).

Table 2. *Table presenting the relative importance of each criterion in the genesis of floods in the catchment area studied.*

No.	Criterion	Classes	Risk Level	Reclassification Note	Class Weight	Criterion Weighting Coefficient
1	Elevation	≤10	High	3	0.63	0.446
		10–30	Medium	2	0.26	
		30+	Low	1	0.11	
2	Drainage density	0–1.5	Low	1	0.11	0.068
		1.5–2.5	Medium	2	0.26	
		2.5–4.5	High	3	0.63	
3	Distance to watercourses	≤100	High	3	0.68	0.174
		100–200	Medium	2	0.21	
		200+	Low	1	0.1	
4	Land use	Vegetation	Low	1	0.11	0.283
		Roads	Medium	2	0.41	
		Buildings	High	3	0.49	

Map of Distance to Rivers

Distance to watercourses is a factor generated by watercourses that highlights the risk of flooding due to the proximity of populations and infrastructure to the channel (Ake *et al.*, 2018). The distance map of the area has three main classes: 0–100 m, 100–200 m, and >200 m. The river class distance with the lowest values (0–100 m) has a high risk of flooding and therefore has a score of 3 (Figure 5). Those with a high distance from the river values (>200 m) have the opposite effect. This last class received a rating of 1 (Table 2).

Land Cover

Land cover has a significant influence on flooding (Magdalena *et al.*, 2017; Rahman *et al.*, 2021). While vegetation promotes the infiltration process, buildings, roads, and other urban development tend to promote runoff, which increases flooding. The land cover map of the Tongo Bassa watershed is shown in Figure 6. It is subdivided into three main classes: built-up areas, which make up 66.12% of the basin area; vegetation (8.81%); and roads, including other spaces, which represent 25% of the catchment area. Scores of 3, 2, and 1 were assigned to each class based on their influence on flooding (Table 2).

Interrelationships and Pairwise Comparisons of Criteria

Knowing that all the criteria do not have the same degree of influence on the flood generation mechanism in the area, it is
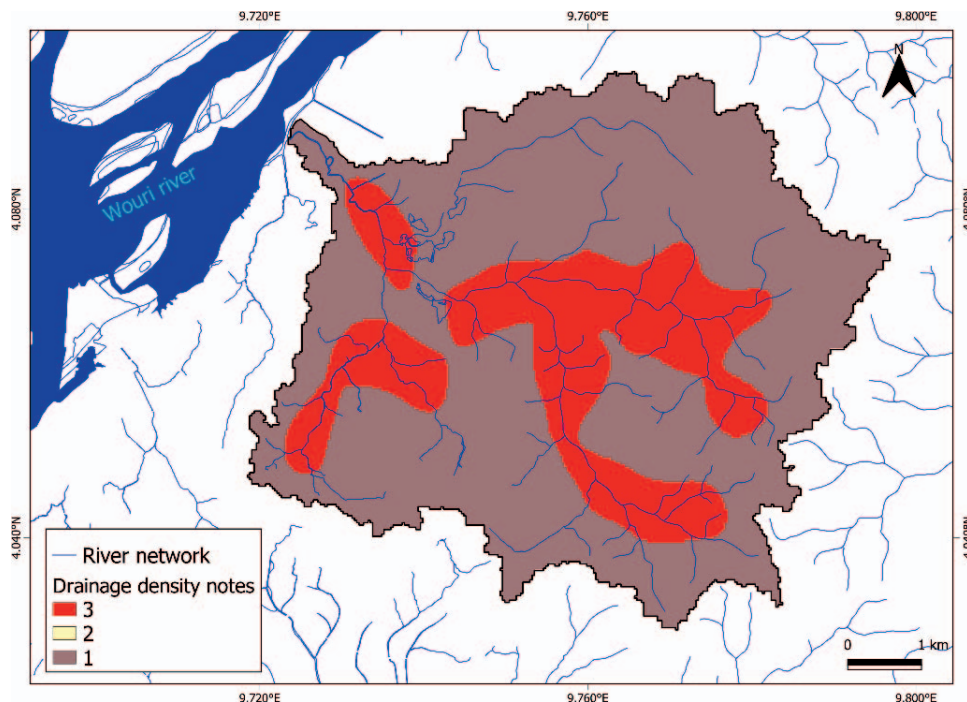

Figure 4. Drainage density map, which presents scores assigned to the density classes of rivers in the watershed to describe the magnitude of flooding (1 = low; 2 = medium; 3 = high).
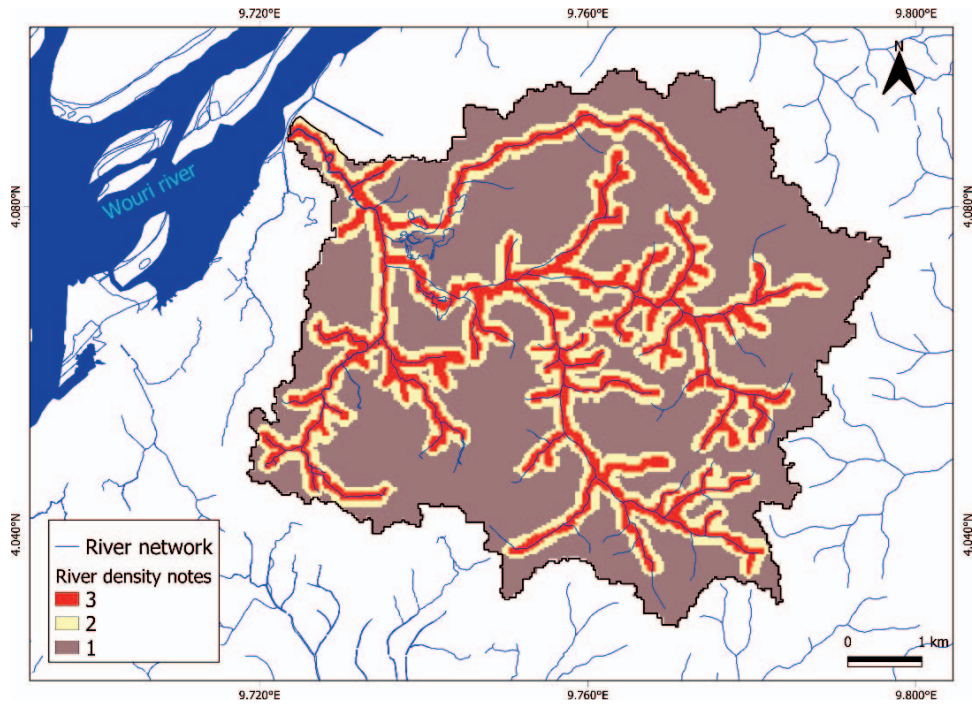
Figure 5. Distance to rivers map, which presents ratings given to classes of distance from population and infrastructure to rivers in the watershed to describe the magnitude of flooding (1 = low; 2 = medium; 3 = high).
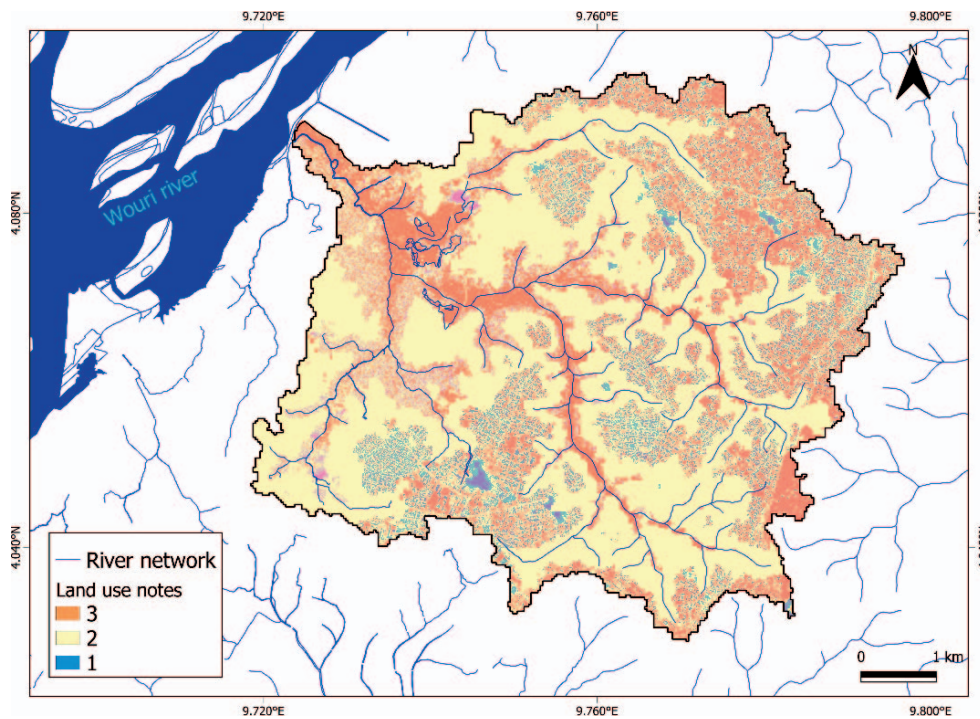

Figure 6. Land-use map, which presents scores assigned to land cover classes in the watershed to describe the extent of flooding (1 = low; 2 = medium; 3 = high).

Table 3. *Characteristic weight of the contribution of the criteria and coherence ratio (*RC*), which demonstrates the coherent character of the reasoning established.*

	Elevation	Land Use	Distance to Watercourses	Drainage Density	Medium (Cp)	$\lambda_{\max}$	IC	RC
Elevation	1	0.2	0.14	7	0.446	4.14	0.045	0.05
Land use	5	1	3	3	0.283			
Distance to watercourses	7	0.33	1	0.33	0.174			
Drainage density	0.14	0.33	3	1	0.068			

necessary to determine the weight of each of the criteria for the studied phenomenon.

Criteria and Influence on the Flood Zone

The determination of a risk area is only possible if each factor is taken independently. The relation of Shaban *et al.* (2001) was applied to the criteria to evaluate the influence of each of them on the susceptibility to floods, and results are summarized in Figure 2. For two parameters separated by a broken arrow, that to which the arrow is pointing is more important relative to the other; conversely, when the line is continuous between two parameters, the one to which the arrow points is less important. The sum of the number of points for each risk factor is recorded in Table 2. The descending order of all these parameters according to their sensitivity to the phenomenon studied is as follows: elevation, land use, distance to rivers, and drainage density.

Weight of Factors

The matrix comparing pairs of parameters was produced to determine the weight of each factor (Table 3). On this basis, the first line of this matrix shows the importance of elevation compared to the other parameters. Calculating the weights (w) from the eigenvectors of the classification matrix revealed that the minimum value of 0.068 corresponds to the weight of drainage density and the maximum value of 0.446 corresponds to the weight of elevation (Table 3). Thus, the density of drainage is considered to be the least important factor in the process of generating floods, and the relief, in particular, the elevation, is the most important.

Consistency Report

The consistency ratio was used to check the consistency of judgments. In this study, the random index (*AI*) and coherence index (*CI*) values for the four (4) parameters were respectively 0.9 and 0.045 for a coherence ratio of the order of 0.05 or 5% (Table 3). This last value is less than 10%, which proves that the hierarchical matrix is acceptable (Elkhrachy, 2015). This coherence ratio value is higher than that obtained by Hammami *et al.* (2019), *i.e.* 0.013 (1.3%), and lower than those of Kazakis, Kougias, and Patsialis (2015) and Ake *et al.* (2018), with values of 0.08 (8%) and 0.07 (7%), respectively, obtained within the framework of the mapping of floodplains on the one hand and the potential recharge of groundwater on the other hand. However, these values vary depending on the number of parameters used.

Flood Risk Map

The mapping of areas at risk of flooding is linked to the values of the factor weights associated with the respective scores of the different maps of the different criteria (Hammami *et al.*, 2019). It was established in a GIS according to Equation (5). Table 3 shows the weight of each criterion, which reflects its estimated contribution to flooding in the watershed according to the model: elevation (44.6%), land cover (28.3%), distance to waterways (17.4%), and drainage density (6.8%). The flood risk index values thus obtained were then classified. The higher is the value, the more susceptible is the area to the risk of flooding. Three classes of flood risk, ranging from a low-risk class to a high-risk class, were distinguished (Figure 4). The areas at high risk of flooding occupied 5.7 km^2 of the surface area or 13.57% of the total surface of the catchment area. Areas at medium risk of flooding occupied 8.3 km^2 of surface area or 19.76% of the total surface of the catchment area. Areas at low risk of flooding occupied 28 km^2 of surface area or 66.67% of the total surface of the catchment area.

Model Validation

Historical data and flood points collected in the field after the 21 August 2020 flood event were used to validate the hierarchical multicriteria analysis model established in this study (Figure 7). The sensitivity analysis of the model consisted of checking the sensitivity of the results to changes in the weights of the criteria considered in the analysis. Analysis was done based on the interrelation between the criteria of the model by changing their respective weights. Thus, a combination of $4^4 = 256$ iterations was applied to the criteria in the GIS. The results obtained from these tests were compared with historical records and flood points collected in the field. The order of the parameters, revealed by weight, that best represented the data of the flood points collected in the field after the flooding of 21 August 2020 followed the sequence: elevation, land cover, distance to watercourses, and drainage density.

The city of Douala has more than 60 districts affected by more than four floods during the period 1984–2018, and 12 have experienced nine or more major flood events. These are essentially located in the middle to lower parts of the main watersheds of the city (Bruckmann, *et al.*, 2019). Figure 8 presents the distribution of neighborhoods in the studied watershed and the frequency of major floods in certain neighborhoods from 1990 to 2018. The Makèpè, Pk 8, and Bepanda neighborhoods can be cited as those where not less than six floods were recorded with significant damage. These neighborhoods, where the frequency of flooding is high, are also located in the high-risk areas determined by the multicriteria model. This shows that the flood sensitivity method adopted can predict the probability of an area being flooded quite accurately.

DISCUSSION

The test of Saaty (1980) applied to the present work revealed that the criteria that considerably influence the phenomenon of
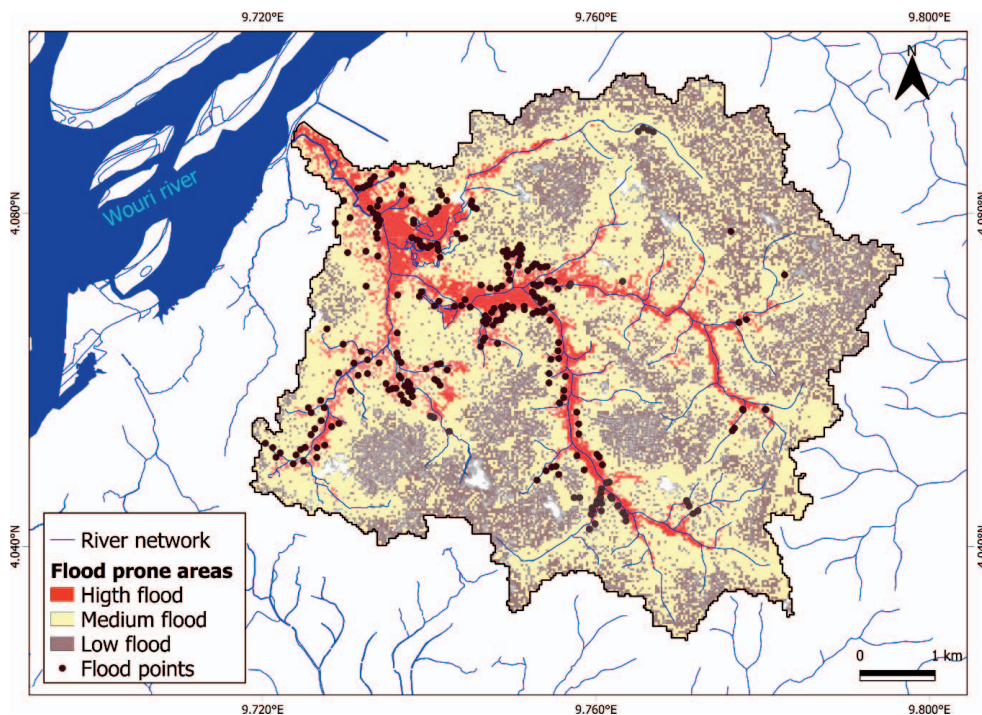
Figure 7. Map of the flood zones, which presents areas at risk of flooding in the Tongo Bassa river basin resulting from the hierarchical multicriteria analysis and best reflecting the flood points collected in the field.

flooding in the watershed of Tongo Bassa are the elevation, the land cover, the distance to the rivers, and drainage density. These criteria were highlighted by Das and Gupta (2021) in the Subarnarekha Basin (India). They used 12 criteria, and their results revealed that the criteria that most influence flood susceptibility in this area are elevation, slope, topographic wetness index, and drainage density. The presented results are consistent, although the number of criteria used is different. Unlike this study site, located in an estuary area and characterized by flat relief, their work was carried out in an area with much more variable relief, and this justifies the larger number of criteria associated with this to better identify flooded areas. The reasoning classifies elevation as the main criterion contributing the most to flooding. Meva'a, Fouda, and Bonglam (2010) indicated that the almost horizontal relief of Douala is one of the main factors amplifying the frequency of floods. Zogning, Tonye, and Tsalefack (2015) added that the relief deserves special attention in Douala because the average elevation is around 27 m. The density of the hydrographic network also favors the diffusion of water in the catchment area. After the Ngonguè, the Kondi, the Moussadi, and the Tongo Bassa Rivers, there are in the study area several other small streams and many artificial drains contributing to feed these main rivers, increasing the risk of flooding. With the reduced number of criteria, criteria contribution rates can be better assessed; this is not the case with a larger number of criteria to integrate into the analysis. Without associating other analyses (statistical and probabilistic), with more certainty, the major contributing element is the topography

of the environment. Thus, a plan for lowland development and flood mitigation should be prioritized among the management options for better adaptation.

The superposition of the 21 August 2020 flood points on the final map revealed that the majority of these points are located in high-risk areas. These areas are generally located near rivers in low elevations (talwegs) and marshy areas regularly occupied by constructions. No flood point was found in the medium- and low-risk zones. This can be explained by the fact that household's channel all their liquid and solid waste, rain water, and household waste toward the rivers, which creates a lot of flooding (Figure 9).

Multicriteria Analysis and Established Reasoning

The multicriteria analysis provides valuable assistance in the geospatial characterization of hydro-geomorphological phenomena involving several parameters or criteria. Coupled with GIS, it makes an undeniable contribution to the knowledge of areas susceptible to flooding in the Tongo Bassa watershed in Douala. This work is the first of its kind to use a wide range of free remote-sensing data (SRTM, Landsat images) to assess the susceptibility of the Tongo Bassa watershed to flooding in a context of global change. In the context of a lack of precise data, these results constitute a first step in the search for an effective solution to the flooding issues in the city of Douala. Indeed, while hydraulic modelling provides valuable knowledge about the spatial distribution of areas at risk of flooding, this approach is very expensive and requires a lot of precise data, material, and financial resources
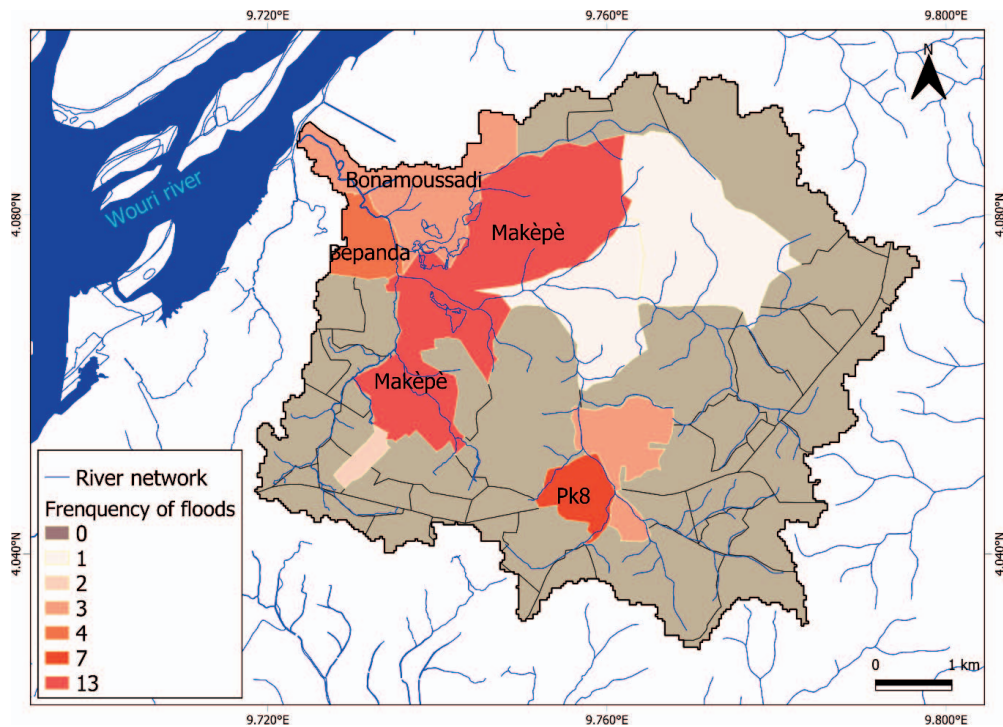
Figure 8. Map of the flooded neighborhoods, which presents the frequency of occasional floods in the catchment area.

that the city of Douala is unable to afford. The hierarchical multicriteria analysis methodology developed in this study can be applied in other watersheds of the city of Douala. The only difference is that the assessment of the criteria that would be included in the flood risk mapping should take into account the inundation points of an experienced flood and the specificities of each catchment area. The tidal phenomenon at the outlet of

the watershed cannot be taken into account as a criterion in this analysis approach. However, this parameter could help to better understand the final result, as is the case in the present study. The criteria should be carefully chosen to avoid redundancies. For example, in the Tongo Bassa watershed, with its almost flat relief, the use of elevation and slope criteria in the analysis model is redundant. Moreover, on sites with

Figure 9. Some anthropogenic activities that promote flooding in the Tongo Bassa watershed in Douala: (A) dumping of household waste into the waters during the flood of 21 August 2020; and (B) construction in low areas close to watercourses.

highly variable relief, the combination of these two parameters is relevant to better identify flood-prone areas (Arabameri *et al.*, 2019; Mahmoud and Gan, 2018; Piri *et al.*, 2019; Srivastava and Bhattacharya, 2006; Tang *et al.*, 2018).

Moreover, when the criteria are too numerous, the risk of inconsistencies in the judgments is too high, and the method of Saaty (1980) can be difficult to implement (Chakhar, 2006). Consuegra, Joerin, and Vitalini (1995) also indicated that this method asks the decision maker to consider all possible comparisons, implicitly assuming that all the criteria considered are perfectly comparable. The standardization of criteria facilitates and makes possible their combination.

Limitations of the Methodology Applied in this Study

The connection of the Tongo Bassa watershed to the Wouri River implies a reverse circulation of water during the rising tide up to a certain level upstream in the river. This increases the size of the flooded surfaces in the watershed. Depending on the rising and falling speeds of the waves and ebbing in the Wouri River, there will be variable proportions of water supply in the catchment area up to a certain elevation from the bottom profile of the river or currents in opposite directions. Field observations allowed us to record the tide about 1.5 km from the outlet of the watershed. This rise in water slows down the flow towards the outlet, which induces an increase in the volumes of water and an increase in the concentration time of the water at the surface. The reverse of the flows in the Wouri River has the consequence of reducing the flow velocity in the drains connected to it by around 16% and increasing the wetted surface by 30% (Ndongo *et al.*, 2015). The contribution of the Wouri waters through the tidal phenomenon is not to be neglected in the process of flooding in the Tongo Bassa watershed. The proposed flood-prone risk area mapping in this present study includes the contribution of the tide but does not indicate its level of exacerbation. The tide would be better taken into account in a hydraulic modelling study. The flood risk areas observed upstream on the rivers on the map could be justified by the barrier effect of the waters at the outlet induced by the tide. The tide prevents the waters from flowing freely at the outlet, thus creating an upwelling of these waters on land with longer stagnation times.

CONCLUSION

This study was based on GIS and hierarchical multicriteria analyses to map the areas at risk of flooding in the watershed of the Tongo Bassa River in Douala. Four criteria were used for the model analysis. The study showed that the main criteria contributing to flooding in order of priority are: elevation, land use, distances to watercourses, and drainage density. According to these results, areas at high risk of flooding were mainly identified in areas with elevations ≤10 m above mean sea level, high drainage density between 2.5 and 4.5 km/km^2, areas close to rivers at distances ≤100 m, and built-up areas at the edge of watercourses in wetlands. The flood points collected directly after the heavy flood of 21 August 2020, helped to validate the flooding risk area map. Three levels of risk were identified: high risk, medium risk, and low risk, where 13.57% of the total area of the watershed is subject to a high risk of flooding. By using historical flood records, the chosen methodology proved to be reliable for the delineation of flood risk areas. This mapping would make it possible to better understand the areas exposed to flooding and could help city managers in planning and implementing management actions aimed at better adapting to flooding in Douala.

LITERATURE CITED

Ahouangan, B.; Houinato, M.; Ahamide, B.; Agbossou, E., and Sinsin, B., 2010. Etude comparative de la productivité de repousses et de la capacité de charge des hémicryptophytes soumises aux feux de végétation dans les parcelles irriguée et non irriguées dans la Réserve Transfrontalière de Biosphère (RTB) du W-Benin. *International Journal of Biological and Chemical Sciences*, 4(2), 479–490.

Ajonina, N.H., 2006. Sedimentology and reservoir potential of sandstones of the Mamfe formation, Mamfe Basin, southeast Nigeria and southwest Cameroon. *Annexe Faculté des Sciences*, 117–130.

Ake, K.J.; Kouame, A.B.; Koffi, J.P., and Jourda, J.P., 2018. Cartographie des zones potentielles de recharge de la nappe de Bonoua (Sud-Est de la Côte d'Ivoire). *Revue des Sciences de l'Eau*, 31(2), 129–144.

Akgun, A. and Turk, N., 2010. Cartographie de la susceptibilité aux glissements de terrain pour Ayvalik (Turquie occidentale) et ses environs par analyse décisionnelle multicritère. *Sciences Environnementales de la Terre*, 61(3), 595–611.

Alfieri, L.; Bisselink, B.; Dottori, F.; Naumann, G.; Roo, A.; Salamon, P.; Wyser, K., and Feyen, L., 2017. Global projections of river flood risk in a warmer world. *Earth's Future*, 5, 171–182. doi:10.1002/2016EF000485

Arabameri, A.; Rezaei, K.; Cerdà, A.; Conoscenti, C., and Kalantari, Z., 2019. Une comparaison des méthodes statistiques et de la prise de décision multicritères pour cartographier la sensibilité aux risques d'inondation dans le nord de l'Iran. *Science de l'environnement Total*, 660, 443–458.

Arnaud, P. and Lavabre, J., 2010. *Estimation de l'aléa pluvial en France métropolitaine*. Versailles, France: Éditions Quae, 158p.

Boum-Nkot, S.N.; Ketchemen-Tandia, B.; Ndje, Y.; Emvouttou, H.; Ebonji, C.R., and Huneau, F., 2015. Origin of mineralization of groundwater in the Tongo Bassa watershed (Douala-Cameroon). *Research Journal of Environmental and Earth Sciences*, 7(2), 29–41.

Bruckmann, L.; Amanejieu, A.; Moffo, M.O.Z., and Ozer, P., 2019. Analyse géohistorique de l'évolution spatio-temporelle du risque d'inondation et de sa gestion dans la zone urbaine de Douala (Cameroun). *Physio-Géo—Géographie Physique et Environnement*, 13, 91–113.

BUCREP (Bureau Central des Recensements et des Etudes de Population), 2010. *La Population du Cameroun en 2010*. Yaoundé, Cameroon: BUCREP.

Bui, D.T.; Tuan, T.A.; Klempe, H.; Pradhan, B., and Revhaug, I., 2015. Spatial prediction models for shallow landslide hazards: a comparative assessment of the efficacy of support vector machines, artificial neural networks, kernel logistic regression, and logistic model tree. *Landslides*, 13, 361–378. doi:10.1007/s10346-015-0557-6

Chakhar, S., 2006. Cartographie Décisionnelle Multicritère: Formalisation et Implémentation Informatique. Paris: Université Paris Dauphine, Ph.D. dissertation.

CRED (Centre for Research on the Epidemiology of Disasters), 2016. *Poverty and Death: Disaster Mortality, 1996–2015*. Brussels, Belgium: Centre for Research on the Epidemiology of Disasters, 22p.

Consuegra, D.; Joerin, F., and Vitalini, F., 1995. Flood Delineation and Impact Assessment in Agricultural Land Using GIS Technology. *In:* Carrara, A. and Guzzetti, F. (eds) *Geographical Information Systems in Assessing Natural Hazards. Advances in Natural and Technological Hazards Research*, vol 5. Dordrecht, The Netherlands: Springer. doi:10.1007/978-94-015-8404-3_9

Daouda, N.; Amidou, K.; Zakari, M.; Abdou, N.N.; Donald, H.F.; Camille, J.; Henri, Z.M.; Oumar, F.M.; Jean-Pierre, V., and Ndam, N.J.R., 2022. Urban flood susceptibility modelling using AHP and GIS approach: Case of the Mfoundi watershed at Yaoundé in the South-Cameroon plateau. *Scientific African*, 15, 9–14.

Das, S. and Gupta, A., 2021. Multi-criteria decision based geospatial mapping of flood susceptibility and temporal hydro-geomorphic changes in the Subarnarekha basin, India. *Geoscience Frontiers*, 12(5), 101206.

Elkhrachy, I., 2015. Cartographie des risques d'inondation soudaine à l'aide d'images satellites et d'outils SIG: Une étude de cas de la ville de Najran, Royaume d'Arabie saoudite (KSA). Autorité nationale pour la télédétection et les sciences spatiales. *The Egyptian Journal of Remote Sensing and Space Sciences*, 18(2), 261–278.

Emmanouloudis, D.; Myronidis, D., and Ioannou, K., 2008. Assessment of flood risk in Thasos Island with the combined use of multicriteria analysis AHP and geographical information system. *Innov Appl Info Agric Environ.*, 2, 103–115.

Fenicia, F.; Kavetski, D.; Savenije, H.H.; Clark, M.P.; Schoups, G.; Pfister, L., and Freer, G., 2013. Propriétés du bassin versant, fonction et représentation du modèle conceptuel: Existe-t-il une correspondance ? *Processus d'Hydrol.*, 28, 2451–2467.

Fernández, D.S. and Lutz, M.A., 2010. Urban flood hazard zoning in Tucumán Province, Argentina, using GIS and multicriteria decision analysis. *Engineering Geology*, 111, 90–98.

Fouda, M. and Meva'a, A.D., 2004. *Rapport des travaux effectués au titre de la carte d'aptitude des sols à l'assainissement individuel de l'agglomération de Douala.* Douala, Cameroon: Société'Assainissement et d'Hydrologie de Grénoble, 38p.

Ghodsipoor, H., 2006. *Discussions on Multi-Criteria Decision.* Tehran, Iran: Amir Kabir Technical University (Tehran Polytechnic), 220p.

Guha-Sapir, D.; Vos, F.; ci-dessous, R., and Ponserre, S., 2011. *Annual disaster statistical review 2010.* Brussels, Belgium: Centre for Research on the Epidemiology of Disasters, 80p.

Hammami, S.; Zouhri, L.; Souissi, D.; Souei, A.; Zghibi, A.; Marzougui, M., and Dlala, 2019. Application of the GIS based multi-criteria decision analysis and analytical hierarchy process (AHP) in the flood susceptibility mapping (Tunisia). *Arab Journal of Geosciences,* 12, 653.

Hirabayashi, Y.; Mahendran, R., and Koirala, S., 2013. Risque d'inondation mondial sous le changement climatique. *Nature Climate Change*, 3, 816–821. doi:10.1038/nclimate1911

IPCC (Intergovernmental Panel on Climate Change), 2012. *Managing the Risks of Extreme Events and Disasters to Advance Climate Change Adaptation. A Special Report of Working Groups I and II of the Intergovernmental Panel on Climate Change.* Geneva, Switzerland: IPCC, 582p.

Issaka, H., 2010. Mise en Carte et Gestion Territoriale des Risques en Milieu Urbain Sahélien à Travers l'Exemple de Niamey. Université de Strasbourg: Strasbourg, France, Ph.D. dissertation, 347p.

Jourda, J.P.; Saley, M.B.; Djagoua, E.V.; Kouame, K.J.; Biemi, J., and Razack, M., 2006. Utilisation des données ETM+ de Landsat et d'un SIG pour l'évaluation du potentiel en eau souterraine dans le milieu fissuré précambrien de la région de Korhogo (nord de la Côté d'Ivoire): Approche par analyse multicritère et test de validation. *Revue de Télédétection*, 5(4), 339–357.

Kazakis, N.; Kougias, I., and Patsialis, T., 2015. Assessment of flood hazard areas at a regional scale using an index-based approach and Analytical Hierarchy Process: Application in Rhodope–Evros region, Greece. *Science of the Total Environment*, 538, 555–563.

Kouassy, K.; Ndam, N.J.R.; Fouépé, T.A.; Zebsa, M., and Mvondo, O.J., 2019. Inondations des 18 et 19 novembre 2016 à Batouri (Est Cameroun): Interprétation des paramètres hydro-météorologiques et contexte historique de l'épisode d'enquête post-événement Hindaoui. *Le Journal du Monde Scientifique*, 2019, 3814962.

Kritikos, T. and Davies, T.R.H., 2011. Analyse décisionnelle multicritères basée sur un SIG pour la cartographie de la susceptibilité aux glissements de terrain dans le nord d'Eubée, en Grèce. *Zeitschrift der Deutschen Gesellschaft für Geowissenschaften*, 162, 421–434.

Lang, M. and Lavabre, J., 2007. *Estimation de la crue centennale pour les plans de prévention des risques d'inondations.* Versailles: Editions Quae, 240p.

Lee, M.J.; Kang, J.E., and Jeon, S., 2012. Application d'un modèle de rapport de fréquence et validation pour la cartographie prédictive de la susceptibilité des zones inondées à l'aide du SIG. *Proceedings of the International Geoscience and Remote Sensing Symposium* (IGARSS) (Munich, Germany, IEEE), pp. 895–898.

Magdalena, R.; Agnoletti, M.; Alaoui, A.; Bathurst, J.C.; Bodner, G.; Borga, M.; Chaplot, V.; Gallart, F.; Glatzel, G.; Hall, J.; Holden, J.; Holko, L.; Horn, R.; Kiss, A.; Kohnova, S.; Leitinger, G.; Lennartz, B.; Parajka, J.; Perdigao, R.; Peth, S.; Plavcova, L.; Quinton, J.N.; Robinson, M.; Salinas, J.L.; Santoro, A.; Szolgay, J.; Tron, S.; van den Akker, J.J.H.; Viglione, A., and Bloschl, G., 2017. Land use change impacts on floods at the catchment scale. Challenges and opportunities for future research. *Water Resources and Research*, 53. doi:10.1002/2017WR020723

Mahmoud, S.H. and Gan, T.Y., 2018. Multi-criteria approach to develop flood susceptibility maps in arid regions of Middle East. *Journal of Cleaner Production*, 196, 216–229. doi:10.1016/j.jclepro.2018.06.047

Malczewski, J., 2006. GIS-based multicriteria decision analysis: A survey of the literature. *International Journal of Geographical Information Science*, 20, 703–726.

Matkan, A.; Shakiba, A.; Pourali, H., and Azari, H., 2009. Flood early warning with integration of hydrologic and hydraulic models, RS and GIS (Case study: Madarsoo Basin, Iran). *World Applied Sciences Journal*, 6, 1698–1704.

Mbaha, J.P.; Olinga, J.M., and Tchiadeu, G., 2013. Cinquante ans de conquête spatiale à Douala: D'héritage colonial en construction à patrimoine socio-spatial vulnérable aux risques naturels. *In: Actes du Colloque des cinquantenaires, La réunification du Cameroun: Bilans, défis et perspective*. Douala, Cameroon: Faculté des Lettres et des Sciences Humaine, Université de Douala, pp. 13–14.

Merwade, V.; Cook, A., and Coonrod, J., 2008. T GIS techniques for creating river terrain models for hydrodynamic mod-eling and flood inundation mapping. *Environmental Modeling & Software*, 23, 1300–1311.

Meva'a, A.D.; Fouda, M., and Bonglam, C.Z., 2010. Analyse spatiale du risque d'inondation dans le bassin versant du Mbanya à Douala, capitale économique du Cameroun. *Proceedings of the Conference on sustainable techniques and strategies for urban water management* (Lyon, France, Novatech), pp. 1–10.

Ndongo, B.; Mbouendeu, S.L.; Tirmou, A.A.; Njila, R.N., and Dalle, J.D.M., 2015. Tendances pluviométriques et impact de la marée sur le drainage en zone d'estuaire: Cas du Wouri au Cameroun. *Afrique Science: Revue Internationale des Sciences et Technologie*, 11(2), 173–182.

Nsegbe, A.; Tchiadeu, G.; Mbaha, J.; Dzalla, G., and Olinga, J., 2014. Douala: une ville d'occupation et d'immigration. *In:* Tchoumtchoua, E. and Dikoumé, A. (eds.), *Douala: histoire et patrimoine*. Yaoundé, Cameroon: Édit, pp. 21–39.

Olinga, O.J.M., 2012. Vulnérabilité des espaces urbains et stratégies locales de développement durable: Etude du cas de la ville de Douala (Cameroun). Mémoire de Master de Géographie, 161p.

Onguene, R.; Pemha, E.; Lyard, F.; Du-Penhoat, Y.; Nkoue, G.; Duhaut, T.; Njeugna, E.; Marsaleix, P.; Mbiake, R.; Jombe, S., and Allain, D., 2014. Overview of tide characteristics in Cameroon coastal areas using recent observations. *Open Journal of Marine Science*, 5(1), 81.

Paquette, J. and Lowry, J., 2012. Modélisation des risques d'inondation et évaluation des risques dans le bassin de la rivière Nadi, Fidji, à l'aide du SIG et de l'AMC. *South Pacific Journal of Natural and Applied Sciences*, 30, 33–43.

PDU (Plan Directeur d'Urbanisme), 2011. *Plan Directeur d'Urbanisme de Douala à l'horizon 2025*. Douala, Cameroon: Édit. République du Cameroun/Communauté Urbaine de Douala, en ligne.

Phonphoton, N. and Pharino, C., 2019. Une modélisation de la dynamique des systèmes pour évaluer les impacts des inondations

sur les services municipaux de gestion des déchets solides. *Waste Management*, 87, 525–536.

Piri, I.; Moosavi, M.; Taheri, A.Z.; Alipur, H.; Shojaei, S., and Mousavi, S.A., 2019. The spatial assessment of suitable areas for medicinal species of *Astragalus* (*Astragalus hypsogeton* Bunge) using the analytic hierarchy process (AHP) and geographic information system (GIS). *Egyptian Journal of Remote Sensing and Space Science*, 22, 193–201. doi:10.1016/j.ejrs.2018.02.003

Pourghasemi, H.R.; Pradhan, B., and Gokceoglu, C., 2012. Application de la logique floue et du processus de hiérarchie analytique (AHP) à la cartographie de la susceptibilité aux glissements de terrain dans le bassin hydrographique de Haraz, en Iran. *Natural Hazards*, 63, 965–996.

Poussin, W.W. and Botzen, J.C., 2014. Facteurs d'influence sur le comportement d'atténuation des dommages causés par les inondations par les ménages. *Environmental Science Policy*, 40, 69–77.

Pradhan, B.; Mansor, S.; Pirasteh, S., and Buchroithner, M.F., 2011. Analyses des aléas et des risques de glissement de terrain dans une zone de captage sujette aux glissements de terrain à l'aide d'un modèle géospatial basé sur des statistiques. *Journal International de Télédétection*, 32(14), 4075–4087.

Rahman, C.; Ningsheng, G.I.; Mahmud, M.M.; Islam, H.R.; Pourghasemi, H.; Ahmad, M.J.; Habumugisha, R.M.A.; Washakh, M.; Alam, E.; Liu, Z.; Han, H.; Shufeng, A., and Ashraf, D., 2021. Flooding and its relationship with land cover change, population growth, and road density. *Geoscience Frontiers*, 12(6), 101224.

Refsgaard, J.C., 1997. Parameterisation, calibration and validation of distributed hydrological models. *Journal of Hydrology*, 198(1–4), 69–97.

Rozos, D.; Bathrellos, G.D., and Skillodimou, H.D., 2011. Comparaison de la mise en œuvre du système d'ingénierie des roches et des méthodes de processus de hiérarchie analytique, sur la cartographie de la susceptibilité aux glissements de terrain, à l'aide d'un SIG: Une étude de cas du comté d'Achaïe orientale du Péloponnèse, en Grèce. *Environnement Terre Science*, 63, 49–63.

Saaty, T.L., 1980. *The Analytic Hierarchy Process*. New York: McGraw-Hill, 287p.

Shaban, M.; Khawlie, R.B.; Kheir, C., and Abdallah, 2001. Évaluation de l'instabilité routière le long d'une route de montagne typique à l'aide d'un SIG et de photos aériennes, Liban-Méditerranée orientale. *Bulletin of Engineering Geology and the Environment*, 60(2), 93–101.

Scheuer, S.; Haase, D., and Meyer, V., 2011. Exploring multicriteria flood vulnerability by integrating economic, social and ecological dimensions of flood risk and coping capacity: From a starting point view towards an end point view of vulnerability. *Natural Hazards*, 58(2), 731–751.

Sinha, R.; Bapalu, G.; Singh, L., and Rath, B., 2008. Analyse des risques d'inondation dans le bassin de la rivière Kosi, au nord du Bihar en utilisant l'approche multiparamétrique du processus de hiérarchie analytique (AHP). *Journal of the Indian Society of Remote Sensing*, 36, 335–349.

Solín, L., 2012. Variabilité spatiale de la vulnérabilité aux inondations des zones urbaines dans les bassins d'amont de la Slovaquie. *Gestion des Risques d'inondation*, 5, 303–320.

Srivastava, P.K. and Bhattacharya, A.K., 2006. Groundwater assessment through an integrated approach using remote sensing, GIS and resistivity techniques: A case study from a hard rock terrain. *International Journal of Remote Sensing*, 27(20), 4599–4620. doi:10.1080/01431160600554983

Tang, Z.; Zhang, H.; Yi, S., and Xiao, Y., 2018. Assessment of flood susceptible areas using spatially explicit, probabilistic multicriteria decision analysis. *Journal of Hydrology*, 558, 144–158. doi:10.1016/j.jhydrol.2018.01.033

Tchiadeu, G. and Ketchemen-Tandia, B., 2009. La ville de Douala face aux changements climatiques. *Actes du Colloque de Yaoundé*, November 2009, 12p.

Tchiadeu, G., and Olinga, O.J.M., 2012. La ville de Douala: Entre baisse des précipitations et hausse des températures. *In:* Bigot, S. and Rome, S. (eds.), *Les climats régionaux: observation et modélisation, 25ème colloque de l'Association Internationale de Climatologie* (Grenoble). Yaoundé, Cameroon: Édit, pp. 727–732.

Tehrany, M.S.; Lee, M.J.; Pradhan, B.; Jebur, M.N., and Lee, S., 2014. Cartographie de la susceptibilité aux inondations à l'aide de modèles statistiques intégrés bivariés et multivariés. *Environnement Terre Science*, 72, 4001–4015.

Youan, Ta.M.; Lasm, T.; Jourda, J.P.; Saley, M.B.; Adja, G.M.; Kouame, K.F., and Biemi, J., 2011. Cartographie des eaux souterraines en milieu fissuré par analyse multicritère: Cas de la région de Bondoukou (Côte-d'Ivoire). *Revue Internationale de Géomatique*, 21(1), 43–71.

Zogning, M.; Tonye, E., and Tsalefack, G., 2015. *Cartography of Flood Prone Areas and Assessment of Flooding Housing in Douala (Cameroon)*. Yaoundé, Cameroon: Université Yaoundé I, 17p.

Zou, Q.; Zhou, J.; Zhou, C.; Song, L., and Guo, J., 2013. Comprehensive flood risk assessment based on set pair analysis-variable fuzzy sets model and fuzzy AHP. *Stochastic Environmental Research and Risk Assessment*, 27, 525–546.